

Synthesis of Cadmium Arsenide Quantum Dots Luminescent in the Infrared

Daniel K. Harris, Peter M. Allen, Hee-Sun Han, Brian J. Walker, Jungmin Lee, and Mounqi G. Bawendi*

Department of Chemistry, Massachusetts Institute of Technology, 77 Massachusetts Avenue, Cambridge, Massachusetts 02139, United States

Supporting Information

ABSTRACT: We present the synthesis of Cd_3As_2 colloidal quantum dots luminescent from 530 to 2000 nm. Previous reports on quantum dots emitting in the infrared are primarily limited to the lead chalcogenides and indium arsenide. This work expands the availability of high quality infrared emitters.

Colloidal quantum dots (QDs) luminescent in the infrared (IR) are an important materials class due to their ability to emit at the telecommunications wavelengths of 1.3 and 1.5 μm and in the second *in vivo* imaging window between 1.1 and 1.35 μm .¹ Previous work on IR quantum dots has been primarily focused on indium arsenide^{2–7} and the lead chalcogenides.^{8–12} We expand the availability of emitters in the IR by demonstrating the synthesis of a size series of nearly monodisperse cadmium arsenide QDs showing well-defined absorption features (Figure 1a) and bright emission.

Bulk Cd_3As_2 is a II–V semiconductor with a narrow band gap. Although there is some debate in the literature regarding the band structure of this material, most experimental results and theoretical predictions suggest an inverted band structure with a band gap of -0.19 eV.^{13–15} Bulk Cd_3As_2 has high carrier concentrations ($2 \times 10^{18} \text{ cm}^{-3}$) and electron mobilities ($10,000 \text{ cm}^2/\text{V}\cdot\text{s}$).¹⁴ In addition, the electron and hole effective masses are $m_e^* = 0.016 m_0$ and $m_h^* = 0.12 m_0$, giving an estimated exciton Bohr radius of ~ 47 nm. Thus, this material is expected to show extreme quantum confinement similar to that observed in PbSe (exciton Bohr radius of ~ 45 nm).¹⁶ The narrow band gap combined with the large exciton Bohr radius enables us to synthesize QDs that show band edge emission over a wide spectral range from 0.6 eV to 2.3 eV (~ 530 – 2000 nm). QDs made from materials with inverted bulk band structure present theoretical challenges because the bands are strongly mixed away from the zone center. The use of a tight binding model to describe the evolution of states in quantum confined negative gap semiconductors has predicted novel properties such as intrinsic surface gap states and an excitonic insulator phase.¹⁷ Thus the synthesis of high quality cadmium arsenide QDs could enable the experimental study of the optical properties of QDs made from a material with an inverted band structure. Much like bulk III–V and II–VI semiconductors, II–V semiconductors are isomorphic and readily form solid solutions,¹⁸ which may enable the development of II–V QD heterostructures and alloys.

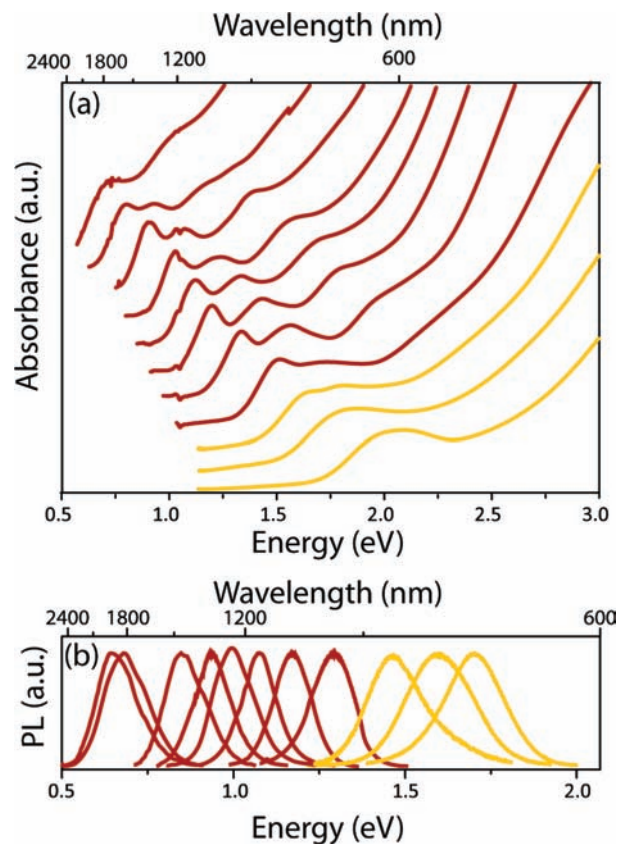


Figure 1. Absorption (a) and corresponding emission (b) spectra from 11 aliquots removed during a single growth. Sizes range from ~ 2 nm for the aliquot emitting at 1.65 eV to ~ 5 nm for the aliquot emitting at 0.65 eV. Yellow curves correspond to aliquots taken before the beginning of the continuous injection. The red curves correspond to aliquots taken during the continuous injection.

Reports of the synthesis of II–V semiconductor nanocrystals have appeared previously,^{19–24} but to our knowledge, the only report of the preparation of Cd_3As_2 QDs used an aqueous method involving arsine gas that produced a solution with absorption and emission features in the visible and fluorescence quantum yields (QY) $< 5\%$.²³

Our approach was inspired by previous reports of the synthesis of Cd_3P_2 QDs from cadmium(II) oleate and

Received: November 19, 2010

Published: March 09, 2011

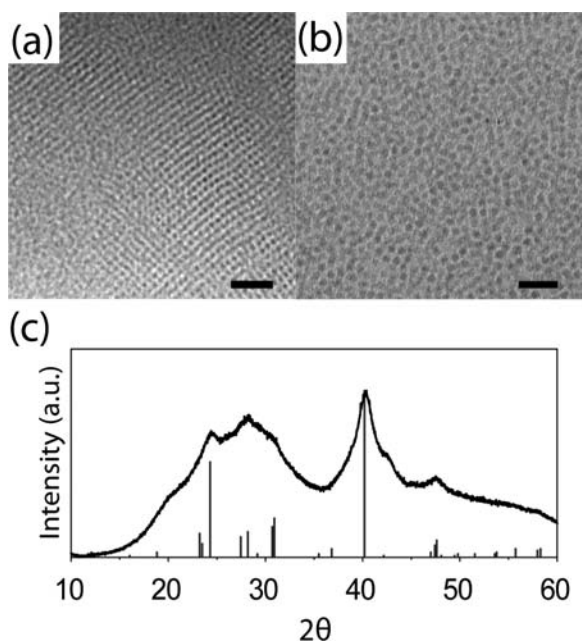


Figure 2. (a) TEM images of 2.2 nm Cd_3As_2 QDs with emission peak at 1.33 eV and (b) 4.5 nm Cd_3As_2 QDs with emission peak at 0.76 eV. Scalebar is 20 nm for both a and b. (c) WAXS of Cd_3As_2 QDs with an emission peak at 1000 nm. The pattern was collected with Cu $K\alpha$ radiation using a helium flow cell. The blue lines represent expected peak values for $\alpha\text{-Cd}_3\text{As}_2$ (PDF #00-056-0233).

tris(trimethylsilyl)phosphine (TMS_3P). These procedures used a single rapid injection of the phosphorus precursor into a hot solution containing cadmium(II) oleate to form Cd_3P_2 QDs. Injection temperature,²⁴ growth time,²⁴ and surfactant concentration²² were modulated to control QD size. Here, we present a two-step procedure that uses an initial fast injection of tris(trimethylsilyl)arsine (TMS_3As) into a solution containing cadmium(II) myristate at 175 °C to form small nuclei followed by the slow, continuous addition of additional TMS_3As to promote growth. This strategy is similar to previous reports of nanocrystal growth by an initial hot injection and subsequent slow injections.⁵

We chose to use the combined fast and slow injections because this method allowed us to maintain narrow emission peaks while precisely tuning the QD size. After beginning the continuous injection, we observed the gradual appearance of higher order absorption features characteristic of samples with narrow size distributions²⁵ and significant narrowing of the emission peak (Figures S1–S2). Furthermore, the slow addition of material allowed us to tune emission peak wavelengths. As expected, the emission peak shifts to the red with increasing particle size (Figure S3).

Transmission electron microscope (TEM) images show narrow size distributions (Figure 2a–b). Measurements show that during the slow injection the particles grow commensurate with the amount of arsenic precursor added. Between the beginning and the end of the continuous addition of the arsenic precursor, the particle volume increased by a factor of ~ 10 . The amount of TMS_3As added during the continuous injection step was 10 times the amount added during the initial injection. Therefore, particle growth is primarily due to the addition of new material to existing nuclei and not an Ostwald ripening mechanism that

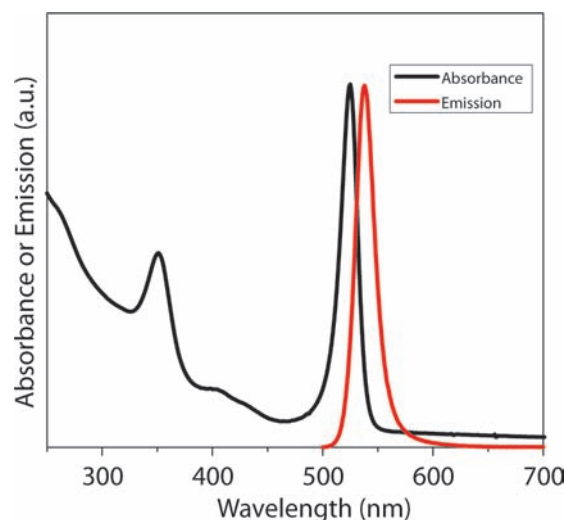


Figure 3. Absorption and emission spectra taken from a solution of Cd_3As_2 clusters 1 min after injection at 130 °C.

would result in a loss of nuclei and a log-normal size distribution.²⁶ ^1H NMR spectroscopy confirms that TMS_3As is completely depleted after exposure to cadmium(II) myristate (Figure S4), eliminating the possibility that the increase in QD size is due to incomplete reaction and particle ripening.

Initial injections at lower temperatures (130 °C) resulted in smaller particles showing well-defined absorption features and narrow emission at wavelengths as blue as 530 nm (Figure 3). These features closely resemble those attributed to Cd_3P_2 magic sized clusters.²¹ With continued heating, the features became less well-defined and shifted to the red, ultimately resembling the spectra of QDs synthesized at 175 °C.

In addition to modulating temperature, we also explored using different surfactant systems. Xie *et al.* reported that by performing the injection at 230–250 °C and varying the concentration of oleic acid, they were able to control the particle size while maintaining narrow emission peaks.²² Although we also observed this behavior, we were only able to produce high quality particles of < 4 nm using this method.

Ultimately, we settled on the two-injection scheme introduced earlier. We injected TMS_3As dissolved in tri-*n*-octylphosphine (TOP) into a solution containing 1-octadecene (ODE) and a 20-fold excess of cadmium(II) myristate at 175 °C. The solution was maintained at 175 °C for 20 min to produce cadmium arsenide quantum dots emitting at 850 nm. After 20 min, a solution of TMS_3As in TOP was added via syringe pump over several hours. Aliquots were taken periodically to monitor the absorption and emission properties. When the emission of the QDs reached the desired wavelength, the addition of TMS_3As was halted and the solution cooled to room temperature. Absorption and emission spectra were taken without purification. When necessary, appropriate blanks were used to collect absorption spectra.

Following growth, the solution was transferred to a glovebox with a nitrogen atmosphere to prepare samples for structural characterization. The growth solution was purified by adding a small amount of acetone to induce flocculation and then centrifuging. The supernatant was discarded, and the resulting precipitate was redispersed in hexane or chloroform. This process was repeated three times before drop-casting onto a

TEM grid or silicon zero-background holder for wide-angle X-ray scattering (WAXS).

The WAXS pattern is consistent with that expected for α - Cd_3As_2 , the stable room temperature phase of Cd_3As_2 (Figure 2c). However, due to the broadening associated with small crystallite size, the α' and β phases cannot be excluded. Application of the Scherrer formula implies an average crystallite size of ~ 2.5 nm. This is consistent with the size observed by TEM. It should be noted that, due to the large unit cell of α - Cd_3As_2 ($a = 12.65$ Å, $c = 25.44$ Å),²⁷ a 2 nm diameter quantum dot has a volume equivalent to roughly one unit cell. Lattice fringes visible by HRTEM confirm the crystalline nature of the particles (Figure S5).

Elemental analysis was performed using energy dispersive X-ray spectroscopy (EDS). The average ratio of cadmium to arsenic was measured to be 3:2 to within experimental error (Table S1).

QYs measured immediately after removal from the growth solution using an integrating sphere ranged as high as 85% for some samples with emission peaks of ~ 900 nm. More typical values ranged from 20% to 60%. The measured QYs decreased substantially for larger particles (Figure S6). This decrease could result from increased rates of multiphonon relaxation for dots with narrower band edges in accordance with the energy gap law.¹⁰ Like most other IR-emitting materials, Cd_3As_2 QDs were found to be air sensitive with QYs declining to $<1\%$ after a few days in ambient conditions (Figure S7a).

A high band gap shell has proven essential for maintaining stability and maximizing the quantum yield for II–VI and III–V semiconductor QDs.²⁸ Cadmium phosphide (Cd_3P_2) was identified as a potential shell material due to its similar crystal structure and larger band gap ($E_g \sim 0.5$ eV).^{18,29} An amount of TMS_3P equivalent to 1–2 monolayers was dissolved in TOP and added dropwise to a solution of ~ 2.5 nm diameter Cd_3As_2 QDs at 175 °C. The addition of TMS_3P resulted in continuous red shifting of the ensemble emission (Figure S7b), which suggests a weaker confinement of the exciton as QD size increases as TMS_3P reacts to form Cd_3P_2 on the dot surface. Elemental analysis of $\text{Cd}_3\text{As}_2(\text{Cd}_3\text{P}_2)$ QDs by EDS confirmed that the dots had an atomic composition of 62.7% cadmium, 10.5% arsenic, and 26.8% phosphorus (Table S2). The ratio of phosphorus to arsenic measured by EDS is consistent with the ratio added to the reaction (3:1 P/As). The shell growth was found to significantly extend the shelf life of Cd_3As_2 QDs stored in ambient conditions (Figure S7a). The shell provided sufficient stability to observe emission after surfactant exchange and dissolution in water, although the QY was $<1\%$ after exchange (Figure S8). During exposure to air or water, the emission peak of the core–shell structure blue shifts. The blue shifted spectrum of a core–shell solution resembles the emission spectrum of the Cd_3As_2 cores (Figure S7c), suggesting that the shell is dissolving or deteriorating. The decrease in QY is consistent with shell deterioration.

In conclusion, a technique for the synthesis of Cd_3As_2 QDs luminescent between 530 and 2000 nm has been developed. Due to the narrow size distribution and bright emission, Cd_3As_2 QDs are well suited to serve as a model system for the fundamental study of quantum confined materials with negative bulk band gaps. In addition, attempts to stabilize the QDs using a passivating shell of Cd_3P_2 have shown promising preliminary results.

■ ASSOCIATED CONTENT

S Supporting Information. Detailed synthetic procedure, Absorption, Photoluminescence, TEM, and EDS are available in

the Supporting Information. This material is available free of charge via the Internet at <http://pubs.acs.org>.

■ AUTHOR INFORMATION

Corresponding Author
mgb@mit.edu

■ ACKNOWLEDGMENT

This work was supported by the US ARO through the ISN (W911NF-07-D-0004) (M.G.B.). This work made use of the MRSEC Shared experimental facilities at MIT, supported by the National Science Foundation (DMR-08-19762). This work also made use of the DCIF (CHE-980806, DBI-9729592). We thank S. Speakman for assistance with WAXS.

■ REFERENCES

- (1) Lim, Y. T.; Kim, S.; Nakayama, A.; Stott, N. E.; Bawendi, M. G.; Frangioni, J. V. *Mol. Imaging* **2003**, *2* (1), 50–64.
- (2) Allen, P. M.; Liu, W. H.; Chauhan, V. P.; Lee, J.; Ting, A. Y.; Fukumura, D.; Jain, R. K.; Bawendi, M. G. *J. Am. Chem. Soc.* **2010**, *132* (2), 470–471.
- (3) Allen, P. M.; Bawendi, M. G. *J. Am. Chem. Soc.* **2008**, *130* (29), 9240–9241.
- (4) Kim, S. W.; Zimmer, J. P.; Ohnishi, S.; Tracy, J. B.; Frangioni, J. V.; Bawendi, M. G. *J. Am. Chem. Soc.* **2005**, *127* (30), 10526–10532.
- (5) Battaglia, D.; Peng, X. *Nano Lett.* **2002**, *2* (9), 1027–1030.
- (6) Cao, Y. W.; Banin, U. *J. Am. Chem. Soc.* **2000**, *122* (40), 9692–9702.
- (7) Guzelian, A. A.; Banin, U.; Kadavanich, A. V.; Peng, X.; Alivisatos, A. P. *Appl. Phys. Lett.* **1996**, *69* (10), 1432–1434.
- (8) Hines, M.; Scholes, G. *Adv. Mater. (Weinheim, Ger.)* **2003**, *15* (21), 1844–1849.
- (9) Yu, W. W.; Falkner, J. C.; Shih, B. S.; Colvin, V. L. *Chem. Mater.* **2004**, *16* (17), 3318–3322.
- (10) Semonin, O. E.; Johnson, J. C.; Luther, J. M.; Midgett, A. G.; Nozik, A. J.; Beard, M. C.; Phys., J. *Chem. Lett.* **2010**, *1* (16), 2445–2450.
- (11) Stouwdam, J. W.; Shan, J.; van Veggel, F. C. J. M.; Pattantyus-Abraham, A. G.; Young, J. F.; Raudsepp, M. *J. Phys. Chem. C* **2006**, *111* (3), 1086–1092.
- (12) Pietryga, J. M.; Werder, D. J.; Williams, D. J.; Casson, J. L.; Schaller, R. D.; Klimov, V. I.; Hollingsworth, J. A. *J. Am. Chem. Soc.* **2008**, *130* (14), 4879–4885.
- (13) Omari, M.; Kouklin, N.; Lu, G.; Chen, J.; Gajdardziska-Josifovska, M. *Nanotechnology* **2008**, *19* (10), 105301.
- (14) Dowgiałło-Plenkiewicz, B.; Plenkiewicz, P. *Phys. Status Solidi B* **1979**, *94* (1), K57–K60.
- (15) Aubin, M. J.; Caron, L. G.; Jay-Gerin, J. P. *Phys. Rev. B* **1977**, *15* (8), 3872.
- (16) Wise, F. W. *Acc. Chem. Res.* **2000**, *33* (11), 773–780.
- (17) Malkova, N.; Bryant, G. W. *Phys. Rev. B* **2010**, *82* (15), 155314.
- (18) Arushanov, E. K. *Prog. Cryst. Growth Charact. Mater.* **1992**, *25* (3), 131–201.
- (19) Green, M.; O'Brien, P. J. *Mater. Chem.* **1999**, *9* (1), 243–247.
- (20) Shen, G. Z.; Bando, Y.; Golberg, D. *J. Phys. Chem. C* **2007**, *111* (13), 5044–5049.
- (21) Wang, R. B.; Ratcliffe, C. I.; Wu, X. H.; Voznyy, O.; Tao, Y.; Yu, K. *J. Phys. Chem. C* **2009**, *113* (42), 17979–17982.
- (22) Xie, R. G.; Zhang, J. X.; Zhao, F.; Yang, W. S.; Peng, X. G. *Chem. Mater.* **2010**, *22* (13), 3820–3822.
- (23) Fojtik, A.; Weller, H.; Henglein, A. *Chem. Phys. Lett.* **1985**, *120* (6), 552–554.
- (24) Miao, S. D.; Hickey, S. G.; Rellinghaus, B.; Waurisch, C.; Eychmuller, A. *J. Am. Chem. Soc.* **2010**, *132* (16), 5613–5615.

- (25) Murray, C. B.; Norris, D. J.; Bawendi, M. G. *J. Am. Chem. Soc.* **1993**, *115* (19), 8706–8715.
- (26) Sugimoto, T. *J. Colloid Interface Sci.* **1978**, *63* (1), 16–26.
- (27) Steigmann, G. A.; Goodyear, J. *Acta Crystallogr., Sect. B* **1968**, *24* (8), 1062–1067.
- (28) Reiss, P.; Protiere, M.; Li, L. *Small* **2009**, *5* (2), 154–168.
- (29) Zdanowicz, W.; Zdanowicz, L. *Annu. Rev. Mater. Sci.* **1975**, *5*, 301–328.